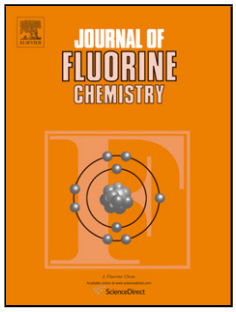

Title: Evaluation of antioxidant activity and cytotoxicity of polyfluorinated diarylacetylenes and indoles toward human cancer cells

Authors: Olga Zakharova, Georgy Nevinsky, Larisa Politanskaya, Dmitry Baev, Ludmila Ovchinnikova, Evgeny Tretyakov

PII: S0022-1139(19)30157-5
DOI: https://doi.org/10.1016/j.jfluchem.2019.109353
Article Number: 109353

Reference: FLUOR 109353

To appear in: *FLUOR*

Received date: 7 May 2019
Revised date: 22 July 2019
Accepted date: 22 July 2019

Please cite this article as: Zakharova O, Nevinsky G, Politanskaya L, Baev D, Ovchinnikova L, Tretyakov E, Evaluation of antioxidant activity and cytotoxicity of polyfluorinated diarylacetylenes and indoles toward human cancer cells, *Journal of Fluorine Chemistry* (2019), https://doi.org/10.1016/j.jfluchem.2019.109353

Evaluation of antioxidant activity and cytotoxicity of polyfluorinated diarylacetylenes and indoles toward human cancer cells

Olga Zakharova[a], Georgy Nevinsky[a,b*], Larisa Politanskaya[b,c*] Dmitry Baev[b,c], Ludmila Ovchinnikova[d], Evgeny Tretyakov[b,c]

[a] Institute of Chemical Biology and Fundamental Medicine, Siberian Branch of Russian Academy of Sciences
Ac. Lavrentiev Ave. 8, Novosibirsk 630090, Russian Federation
[b] Novosibirsk State University
Pirogova Str. 2, Novosibirsk 630090, Russian Federation
[c] N.N. Vorozhtsov Institute of Organic Chemistry, Siberian Branch of Russian Academy of Sciences
Ac. Lavrentiev Ave. 9, Novosibirsk 630090, Russian Federation
[d] Institute of Cytology and Genetics, Siberian Division of Russian Academy of Sciences
Ac. Lavrentiev Ave. 10, Novosibirsk 630090, Russian Federation

∗ Corresponding author. e-mail: nevinsky@niboch.nsc.ru (G. Nevinsky)

∗ Corresponding author. e-mail: plv@nioch.nsc.ru (L. Politanskaya)

Graphical abstract

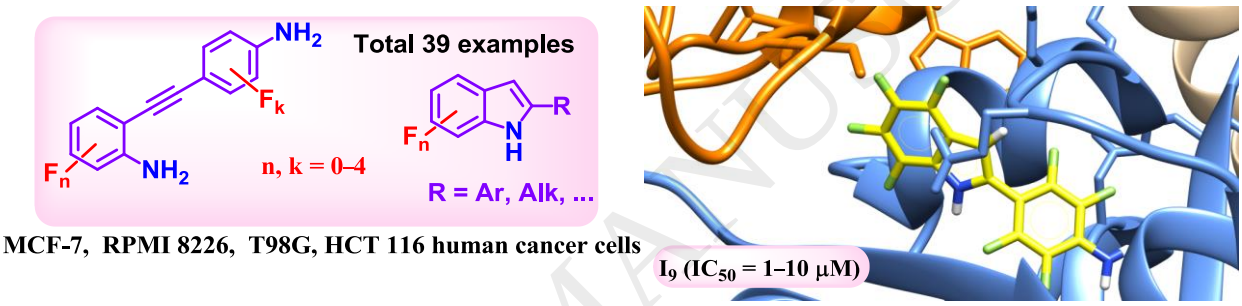

Highlights

- Three polyfluorinated indoles exhibited good potency against human cancer cells.
- DNA fragmentation and Annexin V-FITC/PI staining assays revealed the apoptotic cell death.
- Structure-activity relationship of compounds was illustrated by molecule docking studies
- Compounds good suppress spontaneous and H_2O_2-induced mutagenesis of bacterial cells.

Abstract

A large series of polyfluorinated diarylacetylenes and indoles was evaluated for antitumor activity in MCF-7, RPMI 8226, T98G, HCT 116 human cancer cells and for cytotoxicity effect on HEK-293, WI-38, LMTK, AG 17 normal mammalian cell lines. It was found that with the increased number of fluorine atoms on the benzene ring of the compounds, their cytotoxicity increases, reaching a maximum in case of the perfluorinated structures. Polyfluorinated diarylacetylenes containing three fluorine atoms and trifluoromethyl and amino groups in one aryl ring, inhibit the proliferation of human myeloma RPMI 8226 and human breast cancer MCF-7 cells. Indoles showed more pronounced cytotoxicity as compared with their arylacetylene precursors. Compounds **I9**, **I11**, and **I13** were found to have a high growth-inhibitory activity toward the human cancer cell lines tested, with half-inhibitory concentrations (IC_{50}) of 1–10 μM. The structures of these compounds are characterized by complete fluorination of the

benzene part of the indole core and the presence of an aromatic moiety at the 2nd position of the five-membered ring. Further, DNA fragmentation and Annexin V-FITC/PI staining assays confirm that **I**$_{9}$ – **I**$_{11}$ induce apoptosis. Mutagenic and antioxidant properties of the polyfluorinated indoles and of selected diarylacetylenes were also studied. On a *Salmonella* tester strain, it was demonstrated that the compounds are good antioxidants.

Keywords: Polyfluorinated 2-arylindoles; Polyfluorinated diarylacetylenes; Cytotoxicity; Structure-activity relationship; Mutagenic and antioxidant properties

1. Introduction

Privileged structures, such as the indole class, represent numerous types of molecules that are known to have high binding affinity for various receptors. Because of its presence in a variety of pharmacologically active molecules, the indole moiety is believed to represent the key structural class in the field of drug design and discovery [1]. For instance, the indole nucleus is found in various natural products such as *Catharanthus* alkaloids, well-known mitosis inhibitors [2].

It is general knowledge that substituted 2-arylindoles suppress polymerization of tubulin by selectively binding to the colchicine-binding site in tubulin and thereby stall the cell cycle at the G2/M transition and cause apoptosis [1–4]. In an *in vitro* assay involving breast cancer cell lines, these derivatives showed potency similar to that of vincristine and combretastatin A-4 [3]. Furthermore, 2-arylindoles are inhibitors of polymerization of tubulin [5–7].

These data have aroused substantial interest in the discovery of indole ring-carrying compounds that could be more effective or more specific to tumors or tissues of interest. Introduction of a fluorine atom into biologically active polynuclear aromatic hydrocarbons is known to be effective at modifying their therapeutic efficacy [8]. Because of the specific characteristics of fluorine, such as a small atomic radius, strong electronegativity, and weak polarizability of the C–F bond, substitution of the hydrogen atom by a fluorine atom in functional molecules tends to alter the parent molecule in terms of physicochemical properties (e.g., lipophilicity and electronegativity) and physiological characteristics. The higher activity of the fluorine derivative may be explained by improved pharmacokinetic properties, i.e., greater resistance to metabolic degradation owing to a halogen bond.

In comparison with less fluorinated analogs, benzo-perfluorinated derivatives of 2,2-dimethyl-2,3-dihydro-1*H*-quinolin-4-ones have a stronger cytotoxic effect on RPMI 8226 (human myeloma) cells [9]. A promising antiproliferation activity toward human cancer cells has been detected in polyfluorinated analogs of quinolone based on the skeleton of 3-benzylidene-2-aryl-2,3-dihydroquinolin-4-ones [10].

Indole fluorine derivatives are prominent members of the class of biologically active benzoheterocycles [11]. These observations led to the present study on the cytotoxic and anticancer activities of numerous polyfluorinated 2-arylindoles and their synthetic precursors (polyfluorinated diarylacetylenes), which can also suppress cancer cell proliferation [12,13].

2. Results and discussion

2.1. Synthesis

In Scheme 1 outlined the synthesis of diarylacetylenes **A** and phenylindoles **I** obtained in the present work starting from their corresponding iodoanilines and acetylene derivative. Other investigated compounds were synthesized as described early [14, 15].

2.2. Evaluation of cytotoxicity of polyfluorinated derivatives

All target compounds were tested as growth inhibitors of four human tumorous and four normal mammalian cell lines. Tables 1 and 2 summarize the data on antiproliferative activities of polyfluorinated diarylacetylenes **A** and indoles **I** toward human breast cancer MCF-7 cells, human myeloma RPMI 8226 cells, human glioblastoma T98G cells, human colon carcinoma HCT 116 cells, human embryonic kidney HEK-293 cells, diploid human cell line WI-38, normal mouse fibroblast line LMTK, and Chinese hamster AG 17 cells.

Tables 1 and 2 shows that arylacetylenes have lower cytotoxic activity toward the tested cell lines as compared with the corresponding 2-arylindoles. One also pay attention that nonfluorinated 2-(phenylethynyl)aniline (**A_{18}**) has lower cytotoxicity compared to that manifested by fluorinated diarylacetylenes **A_{10}**–**A_{16}**. For a number of compounds having a phenyl moiety as one of the substituents at the triple bond (**A_{18}**–**A_{13}**), inhibitory action on the growth of human cancer cells increases with the accumulation of fluorine atoms in the second aromatic moiety, reaching its maximum at the complete substitution of all hydrogen atoms with fluorine atoms and the trifluoromethyl group (Table 1, entry 13). For this compound (**A_{13}**) the values of IC_{50} are comparable to those observed for polyfluorinated indoles, most of them far exceed diarylethylene in cytotoxicity.

Indoles **I_9**, **I_{11}**, and **I_{13}** manifested the strongest antiproliferative activity; it was found that their IC_{50} values were lower than 10 μM toward all the human tumor cell lines tested (Table 2, entries 9, 11 and 13). The structures of these compounds are characterized by complete fluorination of the benzene part of the indole core and the presence of an aromatic moiety at the 2nd position of five-membered ring. At the same time, the degree of fluorination of the peripheral aromatic fragment and the presence of the *p*-amino group only slightly effect on the cytotoxic activity of indoles. It follows that the degree of fluorination of the indole benzene moiety has a primary influence on the relative cytotoxicity of the indoles.

The cytotoxic properties of indole **I_{19}** having the benzo-perfluorinated core and a butyl group at position 2, are slightly inferior to those manifested by one of the most active indoles, namely compound **I_9** (Table 2, entries 19 and 9). It is important to note that compounds **I_{20}** and **I_{21}** containing a primary or tertiary alcohol function (CH_2OH or $C(CH_3)_2OH$) at position 2 of the indole nuclear have relatively low activity despite they are structural analogs of the most active benzo-perfluorinated 2-arylindoles (Table 2, entries 20, 21).

Comparison of the IC_{50} values related to different cell lines indicates nonselectivity of the action of all compounds on cancerous and normal cells, similar to the effect of colchicine (Table 2, entry 22). However, a fundamental difference between studied compounds and colchicine is how they induce cell cycle perturbations. The flow cytometric analyses of propidium iodide stained nuclei cells showed that the treating of A-549 cells with indole I_{11} or diarylacetylene A_9 caused a significant accumulation of cells in the G1 phase and a decrease of cells in the G2/M and S phases (see SI). As compared with indole I_{11} and diarylacetylene A_9, colchicine arrest cells at G2/M phase, which mean that it interferes with the mitotic division, that is more promising.

Nevertheless, a malfunctioning of cell cycle control in G1 phase is considered as one of the most critical molecular bases for suppressing of tumor progression, because many of the important processes in the G1 phase play a crucial role in proliferation, differentiation, transformation, and programmed cell death (apoptosis).

2.3. Morphological analysis of apoptosis

Apoptosis is one of the major pathways that lead to the process of cell death. Chromatin condensation, nuclear shrinking and fragmented nuclei are known as classic characteristics of apoptosis. To quantify the apoptotic effect of one of the most active compound **I$_9$**, Annexin V-FITC/Propidium Iodide staining assay was carried out. This study facilitates the detection of necrotic cells (**Q1**-FITC-/PI+); late apoptotic cells (**Q2**-FITC+/PI+); live cells (**Q3**-FITC-/PI-) and early apoptotic cells (**Q4**-FITC+/PI-). In **I$_9$**-treated cells, the annexin V/PI subpopulation increased substantially compared with that in cells treated with DMSO (Fig. 1). According to the data presented in Table 3, the apoptotic population (Q4) increased after incubation of the cells with **I$_9$** compared to the control group treated with DMSO. This assay reveals that compound **I$_9$** shows apoptosis with an increment in early apoptotic cells [control (11.6%), **I$_9$** (35.3%)].

Apoptosis was also assessed by electrophoresis of extracted genomic DNA from cells. Endonuclease mediated cleavage of nuclear DNA results in the formation of oligonucleosomal DNA fragments a biochemical hallmark of apoptosis in many cell types [16]. DNA laddering assay was performed with RPMI 8226 cells by treatment of indoles **I$_9$**–**I$_{11}$** at 7.5 μM concentration for 72 h, then the genomic DNA was isolated and electrophoresis in a 1.8% agarose gel. The tested compounds induce DNA fragmentation which is observed as characteristic ladder pattern in RPMI 8226 cells, while no laddering was observed in control cells (DMSO) indicating that **I$_9$**–**I$_{11}$** induce apoptotic cell death (Fig. 2).

2.4. Docking analysis

As it was mentioned in the introduction, substituted 2-arylindoles are known to suppress polymerization of tubulin. Based on this assumption, we tried to link the observed cytotoxic properties of indoles and acetylenes with their structure when it is placed in the binding site of tubulin by molecular docking. Despite the fact that this study is purely speculative, it, in our opinion, could help to understand the cause of changes in the cytotoxic properties of 2-arylindoles when fluorine atoms are introduced into their structure. Compounds **A$_{13}$** and **I$_9$**, **I$_{11}$**, and **I$_{13}$**, which manifested the highest cytotoxicity, as well as nonfluorinated compounds **A$_{18}$** and **I$_{18}$** (for comparison) were chosen for molecular docking study.

Tubulin can bind with various cytostatic drugs, leading to the stabilization of the microtubules of the cytoskeleton of tumor cells, which leads to disruption of the cell cycle and mitosis. There are three types of cytostatics with different binding sites on the surface of tubulin: similar to colchicine, vinblastine and paclitaxel (taxol). As a result of execution of the docking scoring function, the following values of the docking scores of the tested compounds with tubulin in binding sites were obtained (Table 4).

Indole derivatives that are most active in terms of cytostatic activity show the lowest docking score in the binding site of colchicine, although conformations that can be incorporated into other binding sites are possible. However, the interaction of these compounds with the binding sites of vinblastine and taxol seems less likely, due to the significantly larger sizes of vinblastine and taxol. For a more detailed study of the possible binding of new derivatives, we performed a pharmacophore analysis, presented in SI.

All these new molecules have potent affinity for tubulin, and this affinity is comparable to that of colchicine in the model in question. The colchicine-binding site is formed by the B chain of tubulin at the border with the A chain. The colchicine molecule is prone to the formation of a hydrogen bond between the oxygen of the keto-group of its seven-membered ring and the hydrogen of the amino group of chain A Val181 of tubulin. Within the hydrophobic cavity of the binding site, the colchicine molecule is stabilized by hydrophobic interactions of the π-system of the trimethoxyphenyl moiety. It is possible that the high theoretical affinity of the new derivatives determines hydrophobic interactions of the π-systems of their polyfluorinated rings, which can be got inserted into the hydrophobic pocket of the binding site just as the trimethoxybenzyl cycle of colchicine can. It is also possible that C–F groups play an important role in the formation of very weak interactions both with polar protons and the highly electronegative atoms of amino acid residues that are capable of stabilizing the molecules of these new compounds in the binding site (Fig. 3).

An interesting feature of the new compounds is the possible deeper placement of their polyfluorinated aromatic rings into the hydrophobic pocket of the binding site as compared to colchicine. The compound with the highest theoretical affinity, **I$_9$**, possibly engages in a weak interaction (via its C–F group of the indole ring) with the chain A amino acid residue Val181, which is key for colchicine binding. The amino group of the aniline ring of this molecule can serve as a proton donor for the oxygen of the chain B amino acid residue Val238, forming a hydrogen bond. The trifluoromethyl group in compound **A$_{13}$** is capable of stabilizing the molecule deep in the pocket of the binding site, forming weak interactions via fluorine with the already mentioned oxygen atom of the chain B amino acid residue: Val238. It is also possible for this compound to form a hydrogen bond between the proton of the amino group and the oxygen atom of the chain B amino acid residue Asp251, which can form a weak interaction with one of the C–F groups of the polyfluorinated aromatic ring.

The effect of polyfluorination of aromatic cycles in these compounds on their ability to bind to tubulin is noteworthy. If we compare the calculated spatial configurations of compounds **I$_{18}$** and **A$_{18}$** in the binding site of tubulin with those of their polyfluorinated analogs **I$_9$** and **A$_{13}$**, it becomes apparent that numerous C–F groups allow **I$_9$** and **A$_{13}$** molecules to be positioned deep in the hydrophobic binding site. Compounds **I$_{18}$** and **A$_{18}$** can occupy only the central region of the binding site by means of one of their aromatic rings; this arrangement appears to be insufficient for effective binding to tubulin (Fig. 4).

2.5. Antioxidant properties of of polyfluorinated derivatives

Some biologically active compounds interacting with many cell targets (which is true of indoles) can be polyfunctional and possess cytoprotective properties, or conversely, can be mutagenic or carcinogenic. Evidently, drugs are more successful when they are not mutagenic at

least at the therapeutic concentrations. The *Salmonella* Typhimurium TA102 strain is widely used both for evaluation of mutagenicity of different compounds, including fluorinated arenes, and for detection of antioxidant properties, judging by suppression of spontaneous mutagenesis in this strain and by a decrease in the mutagenicity of oxidants (H_2O_2) [9,17–19]. The mutagenic activity of compounds **A** and **I** was estimated by the Ames test [20] based on *S.* Typhimurium TA102 [21]. Mutagenicity in the Ames test is assessed by computing the frequency of reversion from histidine auxotrophy to prototrophy under the influence of the substance being tested. The mutation induction in the Ames test is estimated by calculating the frequency of reversion from histidine auxotrophy to prototrophy in response to the substance under study [20,21].

The data on the four analyzed polyfluorinated diarylacetylenes and 13 indoles are summarized in Table 5.

It is noteworthy that 15 of 17 compounds had comparable potency (IC_{50} values 0.43–1.34 μM) in suppressing the spontaneous appearance of mutants, whereas two indoles (**I_{12}** and **I_{20}**) turned out to have lower values (Table 5). Fig. 5 shows the representative data on compounds **I_{12}** and **I_{15}**. These compounds differ primarily in a set of substituents on the peripheral aromatic ring. Perfluorinated structure **I_{12}**, containing a para-amino group, had a more pronounced antioxidant effect as compared to that of compound **I_{15}**. Along with compound **I_{12}**, indole **I_{20}** (containing a tertiary alcohol function in its structure) also has low IC_{50} (μM): 0.22 (**I_{12}**) and 0.34 (**I_{20}**). Meanwhile, perfluorinated structure **A_{12}** was found to have the lowest IC_{50} (0.72 μM) among the diarylacetylenes under study. Thus, perfluorinated compounds possess more pronounced cytotoxic and antioxidant activities in comparison with their less fluorinated analogs.

Some antioxidant compounds can efficiently decrease the mutagenic effect of H_2O_2. [9,17–20]. In the Ames test, H_2O_2 was added to TA102 cells at the optimal concentration, 3 mM, and the concentrations of test compound were varied (Fig. 5). At relatively low concentrations (0.028–0.079 μM), all 16 fluorinated derivatives effectively suppressed the H_2O_2-dependent formation of mutants: from 138% to 100% of revertants (the number of revertants observed in the control group without H_2O_2 was set to 100%). Compound **I_{15}** was found to have remarkably higher IC_{50}: 0.25 μM (Table 5). The concentrations corresponding to a decrease in the emergence of mutants from 100% to 50% in the presence of H_2O_2 varied from 0.13 to 1.1 μM, and the lowest IC_{50} was observed for **I_{20}** (0.13 μM) and **I_{12}** (0.16 μM; Table 5). These data indicate that all 17 compounds analyzed are not mutagenic themselves and can effectively decrease the magnitude of spontaneous mutagenesis and the mutagenic effect of H_2O_2.

Trolox (6-hydroxy-2,5,7,8-tetramethylchroman-2-carboxylic acid) is a water-soluble analog of vitamin E, it is often used in biological or biochemical applications to reduce oxidative stress or damage, as well as a standard in determination of the antioxidant properties of new compounds. Previously, we found that at low concentrations (0.3 μM) control trolox suppressed the t-BuO_2H-dependent formation of mutants only for 8.8 % (decrease from 100 to 91.2%) of revertants in the Ames test [21]. Herewith the most active indole **I_{12}** at the same concentration (0.3 μM) suppressed the H_2O_2-dependent formation of mutants from 100 to 40% (Fig. 5, A). Thus, it can be estimated that at concentration 0.3 μM compound **I_{12}** protects cells ~7-fold better than trolox (Table 5). On the average the active indole compounds can be compared or more active then α-tocopherol succinate (Fig. 6).

Comparison of the results on biological testing of polyfluorinated diarylacetylenes and indoles leads to the following observations.

Among 18 compounds of group **A** (diarylacetylenes) studied regarding suppression of the growth of cancerous and normal cells, only 4 compounds were analyzed in experiments on antioxidant activity (**A**$_2$, **A**$_5$, **A**$_{10}$, and **A**$_{12}$). In terms of growth suppression of tumorous and normal cells, **A**$_{10}$ and **A**$_{12}$ have to some extent lower IC_{50} values (6–42 μM) in comparison with compounds **A**$_2$ and **A**$_5$ (35 to >75 μM, Table 1). At the same time, their abilities to suppress the appearance of spontaneous and H_2O_2-dependent mutants were very similar (Table 5).

Among the 21 compounds of group **I** (indoles), only 13 compounds were tested in the experiments on antioxidant activity. The maximum capacity for suppressing the growth of cancerous and normal cells was revealed for compounds **I**$_9$ (1–10 μM), **I**$_{11}$ (1–5 μM), and **I**$_{13}$ (5–35 μM, Table 2). Antimutagenic activity of these three compounds was detected at their lower (comparable) concentrations: 0.71 μM (**I**$_9$), 0.76 μM (**I**$_{11}$), and 0.94 μM (**I**$_{13}$). Of note, the compound **I**$_{12}$ and **I**$_{20}$ (Table 5) having the maximum antioxidant activity suppressed the growth of various cancerous and normal cells remarkably worse than did compounds **I**$_9$, **I**$_{11}$, and **I**$_{13}$: **I**$_{12}$ (6 to >75 μM), and **I**$_{20}$ (29–57 μM, Table 2).

Because none of the compounds enhanced the spontaneous mutagenesis, and all effectively suppressed the mutagenic effect of H_2O_2, they can be considered effective antioxidants. In addition, the 50% decrease in spontaneous and H_2O_2-dependent mutagenesis of bacterial cells was observed at significantly lower concentrations (Table 5) than those exerting a detectable effect on tumor cells (Tables 1 and 2).

In the case of compounds subjected to the analysis of cell protection from spontaneous and peroxide-dependent mutagenesis, the average IC_{50} values were calculated for suppression of the growth of all tumorous and noncancer cells. Then, correlation coefficients between these IC_{50} values of protection from revertant formation and IC_{50} values in experiments with spontaneous and H_2O_2-dependent mutagenesis were calculated (0.34 and 0.32, respectively). The correlation coefficients (0.32–0.34) turned out to be quite low. This means that there is no strict dependence between the antioxidant properties of these compounds and their ability to suppress the growth of cancer cells. The relatively low correlation coefficients may be explained as follows: in addition to interacting with various oxidants in cells, these compounds can in different ways interact with cells and with their various components, including proteins and enzymes, important for the growth of cells.

3. Conclusions

In conclusion, this study revealed that polyfluorinated 2-arylindoles are an interesting class of compounds with high antiproliferative activity toward four cancer cell lines: MCF-7, RPMI 8226, T98G, and HCT 116. The series of *in vitro* experiments showed that benzo-perfluorinated indoles **I**$_9$, **I**$_{11}$, and **I**$_{13}$ have prominent G1-targeting anticancer effects. Furthermore, DNA fragmentation and Annexin V-FITC/PI staining assays revealed that indoles **I**$_9$–**I**$_{11}$ induced the apoptotic cell death. Additionally, indoles exert strong antioxidant action on bacterial cells in the presence or absence of H_2O_2. Generally, it was shown that that fluorinated 2-arylindoles have more pronounced cytotoxic, antioxidant, and antimutagenic properties as compared with their non-fluorinated analogs.

4. Experimental section

4.1. General experimental procedures

All solvents were purified by standard procedures. The starting polyfluorinated iodoanilines were synthesized according to previously described methods [22,23]. Other chemicals were obtained from commercial sources and were used without further purification. Preparative TLC was performed on Merck precoated silica gel 60 PF_{254} containing gypsum. Visualization of the developed chromatograms was performed by means of UV light. NMR spectra were recorded on Bruker Avance-300 (300.13 MHz for ^{1}H and 282.37 MHz for ^{19}F), Bruker Avance-400 (400.13 MHz for ^{1}H) and DRX-500 (500.13 MHz for ^{1}H and 125.76 MHz for ^{13}C) spectrometers. $CDCl_3$ and acetone-d_6 served as solvents, with residual $CHCl_3$ (δ_H = 7.26) or $CDCl_3$ (δ_C = 77.0) and acetone (δ_H = 2.15) or acetone-d_6 (δ_C = 28.6 and 205.0) acting as internal standards. C_6F_6 (δ_F = 163.0) was used as an external reference for recording ^{19}F NMR spectra. ^{13}C NMR spectra were recorded with C–H spin decoupling. Masses of molecular ions were determined by HRMS on a DFS Thermo scientific instrument (EI, 70 eV). Melting points were recorded on a Mettler-Toledo FP81 Thermosystem apparatus. Elemental analyses were performed on a Euro EA-3000 CHNS analyzer, or on Carlo Erba 1106 CHN elemental analyzer. The IR spectra were recorded on a Bruker Vector 22 spectrometer. The Raman spectrum was recorded on Ramanscope Senterra (25 mV, 785 nm).

4.1.1 Synthesis of phenylethynylanilines A; General Procedure

To a solution of 2,3,4-trifluoro-6-iodoaniline [or *o*-iodoaniline] (1 mmol) and ethynylbenzene (150 mg, 1.5 mmol) in dry MeCN (10 mL) in a Schlenk flask under argon $Pd(PPh_3)_2Cl_2$ (28 mg, 0.04 mmol), CuI (17 mg, 0.09 mmol) and Et_3N (3 mL) were added. The reaction mixture was stirred at 60 °C for 3 h. Then, the mixture was allowed to cool down to r.t., and CH_2Cl_2 (10 mL) was added. The mixture was poured into H_2O (20 mL) and extracted with CH_2Cl_2 (3 × 50 mL). The combined organic layers were washed with H_2O (20 mL) and dried ($MgSO_4$). After evaporation of the solvent *in vacuo*, the crude product was purified by preparative TLC to obtain the target product.

4.1.1.1 2,3,4-Trifluoro-6-(phenylethynyl)aniline (A_{16})

Yellowish solid; yield: 210 mg (84%); R_f = 0.58 (EtOAc/hexane, 1:10); mp 61.8–62.7 °C. IR (KBr): 3504, 3399, 3070, 2926, 2854, 1642, 1589, 1523, 1477, 1442, 1387, 1318, 1283, 1241, 1203, 1155, 1070, 1009, 913, 868, 760, 690, 570, 524 cm^{-1}. Raman: 2209 (vs), 1596, 1387, 1094, 998 cm^{-1}. ^{1}H NMR (300 MHz, $CDCl_3$): 7.54–7.51 (m, 2 H, H_m), 7.38–7.36 (m, 3 H, H_p + H_o), 6.98 (ddd, J (H^5,F^4) = 10.3 Hz, J (H^5,F^3) = 7.7 Hz, J (H^5,F^2) = 2.2 Hz, 1 H, H^5), 4.25 (s, 2 H, NH_2). ^{13}C NMR (125.8 MHz, $CDCl_3$): δ = 142.9 (ddd, ^1J (C^4,F^4) = 239.3 Hz, ^2J (C^4,F^3) = 10.8 Hz, C^4), 140.9 (ddd, ^1J (C^3,F^3) = 251.8 Hz, ^2J (C^3,F^2) = 16.5 Hz, ^2J (C^3,F^4) = 13.4 Hz, C^3), 140.1 (ddd, ^1J (C^2,F^2) = 242.2 Hz, ^2J (C^2,F^3) = 12.4 Hz, C^2), 134.5 (d, ^2J (C^1,F^2) = 10.6 Hz, C^1), 131.6 (s, C^{10}), 129.0 (s, C^{12}), 128.6 (s, C^{11}), 122.4 (s, C^9), 114.0 (dd, ^2J (C^5,F^4) = 19.2 Hz, ^3J (C^5,F^3) = 3.2 Hz, C^5), 103.4 (m, C^6), 96.1 (m, C^7), 82.9 (m, C^8). ^{19}F NMR (282 MHz, Acetone-d_6): δ = –150.9 (dd, J (F^4,F^3) = 21.6 Hz, J (F^4,H^5) = 10.3 Hz, 1 F, F^4), –156.3 (dm, J (F^2,F^3) = 20 Hz, J (F^2,H^5) = 2.2 Hz, 1 F, F^2), –159.2 (m, J (F^3,F^4) = 21.5 Hz, J (F^3,F^2) = 20 Hz, J (F^3,H^5) = 7.7 Hz,

1 F, F^3). HRMS (EI): *m/z* $[M]^+$ calcd for $C_{14}H_8F_3N$: 247.0603; found: 247.0602. Anal. Calcd for $C_{14}H_8F_3N$: C, 68.02; H, 3.26; N, 5.67. Found: C, 67.89; H, 3.38; N, 5.53.

4.1.1.2. 2-(Phenylethynyl)aniline (A_{18})

Yellowish solid; yield: 150 mg (89%); R_f = 0.58 (EtOAc/hexane, 1:5); mp 85.8 °C (decomp.) (86–87 °C [24]). NMR spectra are close to that published in literature [24]. ^{1}H NMR (400 MHz, Acetone-d_6): 7.57–7.55 (m, 2 H, H_m), 7.39–7.35 (m, 3 H, H_p + H_o), 7.28 (dd, J (H^3,H^4) = 7.7 Hz, 1 H, H^3), 7.09 (tm, J (H^5,H^4) ≈ J (H^5,H^6) = 8 Hz, 1 H, H^5), 6.79 (dd, J (H^6,H^5) = 8.2 Hz, 1 H, H^6), 6.60 (tm, J (H^4,H^5) ≈ J (H^4,H^3) = 7.7 Hz, 1 H, H^4), 5.13 (s, 2 H, NH_2). ^{13}C NMR (125.8 MHz, Acetone-d_6): δ = 150.9 (s, C^1), 133.3 (s, C^3), 132.6 (s, C^{10}), 131.1 (s, C^5), 129.9 (s, C^{12}), 129.5 (s, C^{11}), 125.0 (s, C^9), 117.8 (s, C^4), 115.4 (s, C^6), 108.0 (s, C^2), 95.4 (s, C^7), 87.8 (m, C^8). Anal. Calcd for $C_{14}H_1N$: C, 87.01; H, 5.74; N, 7.25. Found: C, 87.24; H, 5.66; N, 7.22.

4.1.2 Synthesis of 2-phenylindoles I; General Procedure

To a solution of **A** (0.5 mmol) in MeCN (3 mL), $PdCl_2$ (24 mg, 0.1 mmol) was added, and the mixture was heated at reflux with stirring for 3 h. The desired product was isolated by TLC.

4.1.2.1 5,6,7-Trifluoro-2-phenyl-1H-indole (I_{16})

Yellowish solid; yield: 118 mg (96%); R_f = 0.50 (EtOAc/hexane, 1:10); mp 160.2–160.4 °C. IR (KBr): 3437, 3089, 1603, 1552, 1523, 1471, 1452, 1400, 1377, 1352, 1313, 1255, 1228, 1184, 1063, 962, 931, 852, 767, 727, 692, 673, 588, 553, 497, 432 cm^{-1}. ^{1}H NMR (300 MHz, Acetone-d_6): 11.15 (s, 1 H, NH), 7.89–7.86 (m, 2 H, H_m), 7.45 (tm, J (H_{ar},H_{ar}) = 7.2 Hz, 2 H, H_o), 7.34 (tt, J (H_{ar},H_{ar}) = 7.2 Hz, 1 H, H_p), 7.25 (m, J (H^4,F^5) = 10.5 Hz, J (H^4,F^6) = 6.7 Hz, J (H^4,H^3) = 2 Hz, 1 H, H^4), 6.91 (dd, J (H^3,F^7) = 3 Hz, J (H^3,H^4) = 2 Hz, 1 H, H^3). ^{13}C NMR (125.8 MHz, Acetone-d_6): δ = 147.8 (dd, ^1J (C^5,F^5) = 237.0 Hz, ^2J (C^5,F^6) = 12.0 Hz, C^5), 142.5 (m, C^2), 139.1 (ddd, ^1J (C^7,F^7) = 247.5 Hz, ^2J (C^7,F^6) = 13.4 Hz, ^3J (C^7,F^5) = 2.4 Hz, C^7), 137.4 (ddd, ^1J (C^6,F^6) = 239.3 Hz, ^2J (C^6,F^5) = 18.6 Hz, ^2J (C^6,F^7) = 12.4 Hz, C^6), 132.9 (s, C^8), 130.3 (s, C^9), 129.5 (s, C^{11}), 126.9 (s, C^{10}), 126.6 (m, C^{3a}), 123.1 (dm, ^2J (C^{7a},F^7) = 10.0 Hz, C^{7a}), 102.9 (dd, ^2J (C^4,F^5) = 19.4 Hz, ^3J (C^4,F^6) = 3.7 Hz, C^4), 101.4 (m, C^3). ^{19}F NMR (282 MHz, Acetone-d_6): δ = –145.8 (dd, J (F^5,F^6) = 19.9 Hz, J (F^5,H^4) = 10.5 Hz, 1 F, F^5), –155.7 (dm, J (F^7,F^6) = 19.1 Hz, J (F^7,H^3) = 3 Hz, J (F^7,H_o) = 2 Hz, 1 F, F^7), –170.0 (td, J (F^6,F^5) ≈ J (F^6,F^7) = 19.5 Hz, J (F^6,H^4) = 6.7 Hz, 1 F, F^6). HRMS (EI): *m/z* $[M]^+$ calcd for $C_{14}H_8F_3N$: 247.0603; found: 247.0602. Anal. Calcd for $C_{14}H_8F_3N$: C, 68.02; H, 3.26; N, 5.67. Found: C, 68.21; H, 3.28; N, 5.60.

4.1.2.2 2-Phenyl-1H-indole (I_{18})

Yellowish solid; yield: 67 mg (77%); R_f = 0.61 (EtOAc/hexane, 1:5); mp 189.1–189.6 °C (189–191 °C [25]). NMR spectra are close to that published in literature [25]. ^{1}H NMR (500 MHz, Acetone-d_6): 10.67 (s, 1 H, NH), 7.87–7.85 (m, 2 H, H_m), 7.57 (d, J (H^4,H^5) = 7.9 Hz, 1 H, H^4), 7.45–7.41 (m, 3 H, H_p + H_o), 7.30 (t, J (H^7,H^6) ≈ J (H^7,H_o) = 7.4 Hz, 1 H, H^7), 7.11 (t, J (H^6,H^7) ≈ J (H^6,H^5) = 7.2 Hz, 1 H, H^6), 7.03 (t, J (H^5,H^6) ≈ J (H^5,H^4) = 7.3 Hz, 1 H, H^5), 6.90 (m, 1 H, H^3). ^{13}C NMR (125.8 MHz, Acetone-d_6): δ = 138.7 (s, C^2), 138.3 (s, C^{7a}), 133.5 (s, C^8), 130.1 (s, C^{3a}), 129.7 (s, C^9), 128.2 (s, C^{11}), 125.8 (s, C^{10}), 122.6 (s, C^6), 121.1 (s, C^4), 120.4 (s, C^5), 112.0 (s, C^7), 99.9 (s, C^3). Anal. Calcd for $C_{14}H_1N$: C, 87.01; H, 5.74; N, 7.25. Found: C, 86.98; H, 5.95; N, 7.27.

The other polyfluorinated compounds studied in this work were obtained according to the methods published earlier: **A**$_1$ – **A**$_{12}$ [15], **A**$_{13}$ – **A**$_{15}$, **A**$_{17}$ [22]; **I**$_1$ – **I**$_{12}$ [15], **I**$_{13}$ – **I**$_{15}$, **I**$_{17}$, **I**$_{19}$ – **I**$_{21}$. [14].

4.2. Cell culture

MCF-7, human myeloma RPMI 8226, human glioblastoma cells T98G, human colon carcinoma cells HCT116 and human embryonic kidney cells HEK-293, embryonic lung fibroblasts WI-38 (SV40 transformed), normal mouse fibroblasts LMTK, Chinese hamster AG 17 cells were used.

Cell lines RPMI 8226, MCF-7, T98G, HCT116, HEK-293, WI-38, LMTK, AG-17 were obtained from the Russian cell culture collection (Russian Branch of the ETCS, Russia, St. Petersburg). Cells were cultivated in Iscove's modified Dulbecco's media (Sigma) with 10% FBS (GibcoBRL Co., Gaithersburg, MD), 2 mM L-glutamine (Sigma), 250 mg/mL amphotericin B and 100 U/mL penicillin/streptomycin (GIBCO BRL Co., Gaithersburg, MD). RPMI 8226 cells were cultivated in RPMI 1640 media (Sigma) supplemented with 10% FBS, 2 mM L-glutamine, 250 mg/ml amphotericin B and 100 U/mL penicillin/streptomycin. Cells were grown in a humidified atmosphere of 5% CO_2 in air at 37 ^{o}C and were passaged with 0.05% trypsin-EDTA every 3–4 days.

4.3. In vitro cytotoxicity assay

To evaluate antiproliferative properties of compounds **A** and **I**, the MTT assay (by using 3-(4,5-dimethyl-2-thiazolyl)-2,5-diphenyl-2*H*-tetrazolium bromide) [26] was performed. Briefly, cells were seeded at 2×10^3 cells/well in a 96-well plates in a total volume of 100 μL in IMDM medium supplemented 2 mM L-glutamine (Sigma), 250 mg/mL amphotericin B and 100 U/mL penicillin/streptomycin and 10% FBS. Cells (except for suspension cell line RPMI 8226) were incubated overnight and 1 μL of DMSO solutions of substances with different concentrations were added to each well. After 72-hours incubation at 37 °C, MTT was added to final concentration of 0.5 mg/mL. Three hours later culture medium was removed, MTT formazan crystals were solubilized in 100 μL isopropanol and absorbance was measured at 570 nm in plate reader Multiscan-FS (Thermo Fisher Scientific). The experiments were performed in triplicate and repeated 3÷5 times for each compound per cell line. IC_{50} values reflecting the relative number of living cells normalized to the number of cells treated with 1% DMSO were calculated from dose-response curve using Origin 8.0 software. Topothecan was used as a cell death inducing positive control.

4.4. Annexin V binding assay

In order to determine the apoptosis induced cell death annexin V FITC and propidium iodide staining was performed by using the Annexin V FITC apoptosis detection kit according to manufacturer's protocol (Sigma Aldrich). The cells were treated with concentrations of 7.5 μM compound **I**$_9$ along with the control (DMSO). After 72 h of incubation, the cells were harvested, washed with PBS and stained with Annexin V FITC and propidium iodide. Early and late

apoptotic cells were quantified using Accuri C6 flow cytometer based software (BD Biosciences).

4.5. DNA fragmentation analysis

RPMI 8226 cancer cells were seeded in well plates and incubated for 24 h. After incubation, cells were treated with tested fluorinated compounds at a 7.5 μM concentration for 72 h. Subsequently, cells were collected and centrifuged for 5 min at 4 °C. Pellet was collected and washed with Phosphate buffered saline (PBS), added 200 μL of Lysis buffer (6M GuSCN), 4 μL of mercapthoethanol and incubated for 20 min at 56 °C. Later 280 μL of GuSCN-containing adsorption buffer was added. The binding solution was mixed thoroughly and transferred to the silica spin column. The column was put in a centrifuge, centrifuged for 1 min (13000 rpm), washed twice with buffer (4.5 M GuSCN) and centrifuged again (1 min, 13000 rpm). GuSCN was removed by washing the column with ethanol, containing buffer (500 mkL×2). The column was centrifuged (1 min, 13000 rpm). DNA was eluted with 30 μL of milli-Q water by centrifugation (1 min, 13000 rpm). DNA laddering was determined by 1.8% agarose gel electrophoresis.

4.6. Docking studies

Molecular modeling was carried out in the Schrodinger Maestro visualization environment using applications from the Schrodinger Small Molecule Drug Discovery Suite 2017-1 package [Schrödinger, LLC, New York, NY, 2017]. Three-dimensional structures of the derivatives were obtained empirically in the LigPrep application using the OPLS3 force field [27]. All possible tautomeric forms of compounds, as well as various states of polar protons of molecules in the pH range of 7.0±2.0 were taken into account. X-ray crystallographic models of interaction of colchicine and tubulin with PDB ID 4O2B (resolution of 2.3 Å) [28], vinblastine and tubulin with PDB ID 5J2T (resolution 2.2 Å) [29], dictyostatin and tubulin with PDB ID 5MF4 (resolution 2.3 Å) [30] were used for the calculations. To simulate the possible mechanism of tubulin binding, molecular docking of new compounds to the binding sites of cytostaticshas been performed in the Glide application [31]. The search area for docking was selected automatically, based on the size and physico-chemical properties ofcytostatics. The extra precision (XP) algorithm of docking was applied. Docking was performed in comparison withcytostatics. The three-dimensional structures of cytostatics were obtained in the PubChem database and prepared in the LigPrep application. Non-covalent interactions of compounds in the binding site were visualized using Biovia Discovery Studio Visualizer [Dassault Systèmes BIOVIA, San Diego, 2016] and UCSF Chimera 1.11.2 [32].

4.7. Determination of mutagenicity

In the Ames test, the histidine-dependent strain of *S. typhimurium* TA102 was used, which carries a mutation at the histidine operon [20]. The mutagenic activity of the samples was analyzed by the standard method without metabolic activation [20]. A liquid culture of TA102 was obtained by 16-h growth of cells from a frozen stock at 37 °C in LB medium with penicillin. Then cells were plated on minimal glucose agar, antibiotics and histidine at the density sufficient

to obtain isolated colonies. A separate bacterial colony was inoculated into LB medium (5 mL) containing ampicillin (50 μg/mL) and tetracycline (2 μg/mL), and grown with shaking (130 rpm) for 15 h at 37 °C.

The Ames test was carried out using the described double-layer method [21]. The overnight culture of bacteria (100 μL) containing one of the tested compounds in different concentrations and, if required, 3 mM H_2O_2, were mixed at 42 °C with 2 ml of liquid 0.6% top agar. The mixture was poured onto plates with a minimal medium containing 0.2% glucose and 3% agar, taking care to distribute the mixture uniformly on the surface of the solid agar. The plates were incubated for 48 h at 37 °C, and the revertants were counted. The cells incubated with H_2O_2 in the absence of compounds analyzed were used as positive controls, and the cells grown in the absence of H_2O_2 and antioxidants served as negative controls for the mutation induction. The results are expressed as mean ± standard deviation of at least 3 independent experiments.

Acknowledgments

The work was supported by the Russian Foundation for Fundamental Studies under Grant № 19-53-53003\19. The authors thank the Multi-Access Chemical Service Center SB RAS and Olga Koval for spectral and analytical measurements.

References

[1] S. Lal, T.J. Snape, 2-Arylindoles: a privileged molecular scaffold with potent, broad-ranging pharmacological activity, Cur. Med. Chem 19 (2012) 4828–4837.

[2] A. Brancale, R. Silvestri, Indole, a core nucleus for potent inhibitors of tubulin polymerization, Med. Res. Rev. 27 (2007) 209–238.

[3] D. Kaufmann, M. Pojarova, S. Vogel, R. Liebl, R. Gastpar, D. Gross, T. Nishino, T. Pfaller, E. von Angerer, Antimitotic activities of 2-phenylindole-3-carbaldehydes in human breast cancer cells, Bioorg. Med. Chem. 15 (2007) 5122–5136.

[4] G. De Martino, M.C. Edler, G. La Regina, A. Coluccia, M.C. Barbera, D. Barrow, R.I. Nicholson, G. Chiosis, A. Brancale, E. Hamel, M. Artico, R. Silvestri, New arylthioindoles: potent inhibitors of tubulin polymerization. 2. Structure-activity relationships and molecular modeling studies J. Med. Chem. 49 (2006) 947–954.

[5] R. Gastpar, M. Goldbrunner, D. Marko, E. von Angerer, Methoxy-Substituted 3-Formyl-2-phenylindoles Inhibit Tubulin Polymerization J. Med. Chem. 41 (1998) 4965–4972.

[6] B.L. Flynn, E. Hamel, M.K. Jung, One-pot synthesis of benzo[*b*]furan and indole inhibitors of tubulin polymerization, J. Med. Chem. 45 (2002) 2670–2673.

[7] M. Medarde, A.C. Ramos, E. Caballero, R.P.-L. de Clairac, J.L. Lopez, D.G. Gravalos, A.S. Feliciano, Synthesis and pharmacological activity of diarylindole derivatives. Cytotoxic agents based on combrestatins, Bioorg. Med. Chem. Lett. 9 (1999) 2303–2308.

[8] (a) C. Isanbor, D. O'Hagan, Fluorine in medicinal chemistry: a review of anti-cancer agents, J. Fluorine Chem. 127 (2006) 303–319; (b) R.W. Dolbier Jr, Fluorine chemistry at the millennium, J. Fluorine Chem. 126 (2005) 157–163; (c) A.A. Gakh, M.N. Burnett, Extreme modulation properties of aromatic fluorine, J. Fluorine Chem. 132 (2011) 88–93; (d) J. Wang, M. Sanchez-Rosello, J.L. Acen, C. del Pozo, A.E. Sorochinsky, S. Fustero, V.A. Soloshonok, H. Liu, Fluorine in pharmaceutical industry: fluorine-containing drugs introduced to the market in the last decade (2001−2011), Chem. Rev. 114 (2014) 2432−2506.

[9] L.V. Politanskaya, I.P. Chuikov, E.V. Tretyakov, V.D. Shteingarts, L.P. Ovchinnikova, O.D. Zakharova, G.A. Nevinsky, An effective two-step synthesis, fluorescent properties, antioxidant activity and cytotoxicity evaluation of benzene-fluorinated 2,2-dimethyl-2,3-dihydro-1*H*-quinolin-4-ones, J. Fluorine Chem. 178 (2015) 142–153.

[10] L. Politanskaya, T. Rybalova, O. Zakharova, G. Nevinsky, E. Tretyakov, *p*-Toluenesulfonic acid mediated one-pot cascade synthesis and cytotoxicity evaluation of polyfluorinated 2-aryl-2,3-dihydroquinolin-4-ones and their derivatives, J. Fluor. Chem. 211 (2018) 129–140.

[11] E.V. Nosova, G.N. Lipunova, V.N. Charushin, O.N. Chupakhin, Fluorine-containing indoles: Synthesis and biological activity, J. Fluorine Chem. 212 (2018) 51–106.

[12] (a) V.M. Sviripa, W. Zhang, L.M. Kril, A.X. Liu, Y. Yuan, C.-G. Zhan, C. Liu, D.S. Watt, Halogenated diarylacetylenes repress c-myc expression in cancer cells, Bioorg. Med. Chem. Lett. 24 (2014) 3638–3640; (b) V.M. Sviripa, L.M. Kril, W. Zhang, Y. Xie, P. Wyrebek, L. Ponomareva, X. Liu, Y. Yuan, C.-G. Zhan, D.S. Watt, C. Liu, Phenylethynyl-substituted heterocycles inhibit cyclin D1 and induce the expression of cyclindependent kinase inhibitor p21Wif1/Cip1 in colorectal cancer cells, Med. Chem. Commun. 9 (2018) 87–99.

[13] C. Wang, B. Carter-Cooper, Y. Du, J. Zhou, M.A. Saeed, J. Liu, M. Guo, B. Roembke, C. Mikek, E.A. Lewis, R.G. Lapidus, H.O. Sintim, Alkyne-substituted diminazene as G-quadruplex binders with anticancer activities, Eur. J. Med. Chem. 118 (2016) 266–275.

[14] L.V. Politanskaya, I.P. Chuikov, V.D. Shteingarts, Synthesis of indoles with a polyfluorinated benzene ring, Tetrahedron 69 (2013) 8477–8486.

[15] L.V. Politanskaya, V.D. Shteingarts, E.V. Tretyakov, General and efficient synthesis of polyfluorinated 2-aminotolans and 2-arylindoles, J. Fluorine Chem. 188 (2016) 85–98.

[16] A. Kamal, P.S. Srikanth, M.V.P.S. Vishnuvardhan, G.B. Kumar, K.S. Babu, S.M.A. Hussaini, J.S. Kapure, A. Alarifi, Combretastatin linked 1,3,4-oxadiazole conjugates as a potent tubulin polymerization inhibitors, Bioorg. Chem. 65 (2016) 126–236.

[17] O.A. Zakharova, L.I. Goryunov, N.M. Troshkova, V.D. Shteingarts, G.A. Nevinsky, Cytotoxicity of new n-butylamino and sulfur-containing derivatives of polyfluorinated 1,4-naphthoquinone, Eur. J. Med. Chem. 45 (2010) 270–274.

[18] O.A. Zakharova, L.I. Goryunov, N.M. Troshkova, V.D. Shteingarts, G.A. Nevinsky, Cytotoxicity of new alkylamino- and phenylamino-containing polyfluorinated derivatives of 1,4-naphthoquinone, Eur. J. Med. Chem. 45 (2010) 2321–2326.

[19] O.A. Zakharova, L.I. Goryunov, N.M. Troshkova, V.D. Shteingarts, G.A. Nevinsky, Cytotoxicity of new polyfluorinated 1,4-naphtoquinones with diverse substituents in the quinone moiety, Bioorg. Med. Chem. 19 (2011) 256–260.

[20] D.M. Maron, B.N. Ames, Revised methods for the Salmonella mutagenicity test, Mutat. Res. 113 (1983) 173–215.

[21] O.D. Zakharova, T.S. Frolova, Y.V. Yushkova, E.I. Chernyak, A.G. Pokrovsky, M.A. Pokrovsky, S.V. Morozovb, O.I. Sinitsina, I.A. Grigorev, G.A. Nevinsky, Antioxidant and antitumor activity of Trolox, Trolox succinate, and α-Tocopheryl succinate conjugates with nitroxides, Eur. J. Med. Chem., 122 (2016) 127–137.

[22] L.V. Politanskaya, I.P. Chuikov, E.A. Kolodina, M.S. Shvartsberg, V.D. Shteingarts, Synthesis of polyfluorinated ortho-alkynylanilines, J. Fluorine Chem. 135 (2012) 97–107.

[23] L. Politanskaya, E.Tretyakov, *p*-Toluenesulfonic acid induced conversion of fluorinated trimethylsilylethynylanilines into aminoacetophenones: versatile precursors for the synthesis of benzoazaheterocycles, Synthesis 50 (2018) 555–564.

[24] B. Miao, Y. Zheng, P. Wu, S. Li, S. Ma, Bis(cycloocta-1,5-diene)nickel-catalyzed carbon dioxide fixation for the stereoselective synthesis of 3-alkylidene-2-indolinones, Adv. Synth. Catal. 359 (2017) 1691–1707.

[25] Y. Yu, X. Chen, Q. Wu, D. Liu, L. Hu, L. Yu, Z. Tan, Q. Gui, G. Zhu, Synthesis of aryl alkynes via copper catalyzed decarboxylative alkynylation of 2-nitrobenzoic acids, J. Org. Chem. 83 (2018) 8556−8566.

[26] T. Mosmann, Rapid colorimetric assay for cellular growth and survival: application to proliferation and cytotoxicity assays, J. Immunol Methods. 65 (1983) 55–63.

[27] E. Harder, W. Damm, J. Maple, C. Wu, M. Reboul, J.Y. Xiang, L. Wang, D. Lupyan, M.K. Dahlgren, J.L. Knight, J.W. Kaus, D.S. Cerutti, G. Krilov, W.L. Jorgensen, R. Abel, R.A. Friesner, OPLS3: a force field providing broad coverage of drug-like small molecules and proteins, J. Chem. Theor. Comput. 12 (2016) 281–296.

[28] A.E. Prota, F. Danel, F. Bachmann, K. Bargsten, R.M. Buey, J. Pohlmann, S. Reinelt, H. Lane, M.O. Steinmetz, The novel microtubule-destabilizing drug BAL27862 binds to the

colchicine site of tubulin with distinct effects on microtubule organization, J. Mol. Biol. 426 (2014) 1848–1860.

[29] A.B. Waight, K. Bargsten, S. Doronina, M.O. Steinmetz, D. Sussman, A.E. Prota, Structural basis of microtubule destabilization by potent auristatin anti-mitotics, PLOS ONE 11 (2016) 1−14. doi:10.1371/journal.pone.0160890.

[30] C. Trigili, I. Barasoain, P.A. Sanchez-Murcia, K. Bargsten, M. Redondo-Horcajo, A. Nogales, N.M. Gardner, A. Meyer, G.J. Naylor, E. Gomez-Rubio, F. Gago, M.O. Steinmetz, I. Paterson, A.E. Prota, J.F. Díaz, Structural determinants of the dictyostatin chemotype for tubulin binding affinity and antitumor activity against taxane- and epothilone-resistant cancer cells, ACS Omega 1 (2016) 1192−1204. doi:10.1016/j.jmb.2014.02.005.

[31] R.A. Friesner, R.B. Murphy, M.P. Repasky, L.L. Frye, J.R. Greenwood, T.A. Halgren, P.C. Sanschagrin, D.T. Mainz, Extra precision glide: docking and scoring incorporating a model of hydrophobic enclosure for protein−ligand complexes, J. Med. Chem. 49 (2006) 6177–6196.

[32] E.F. Pettersen, T.D. Goddard, C.C. Huang, G.S. Couch, D.M. Greeblatt, E.C. Meng, T.E. Ferrin, UCSF Chimera – a visualization system for exploratory research and analysis, J. Comput. Chem. 25 (2004) 1605–1612.

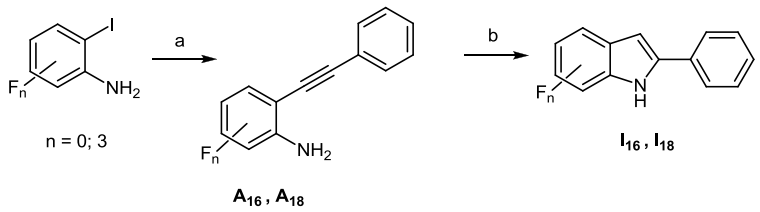

Reagents and conditions: (a) HC≡CPh, $Pd(PPh_3)_2Cl_2$, CuI, Et_3N, MeCN, Ar, 60 °C, 3 h; (b) $PdCl_2$, MeCN, Ar, reflux, 3 h.

Scheme 1. Synthesis of polyfluorinated diarylacetylenes and indoles

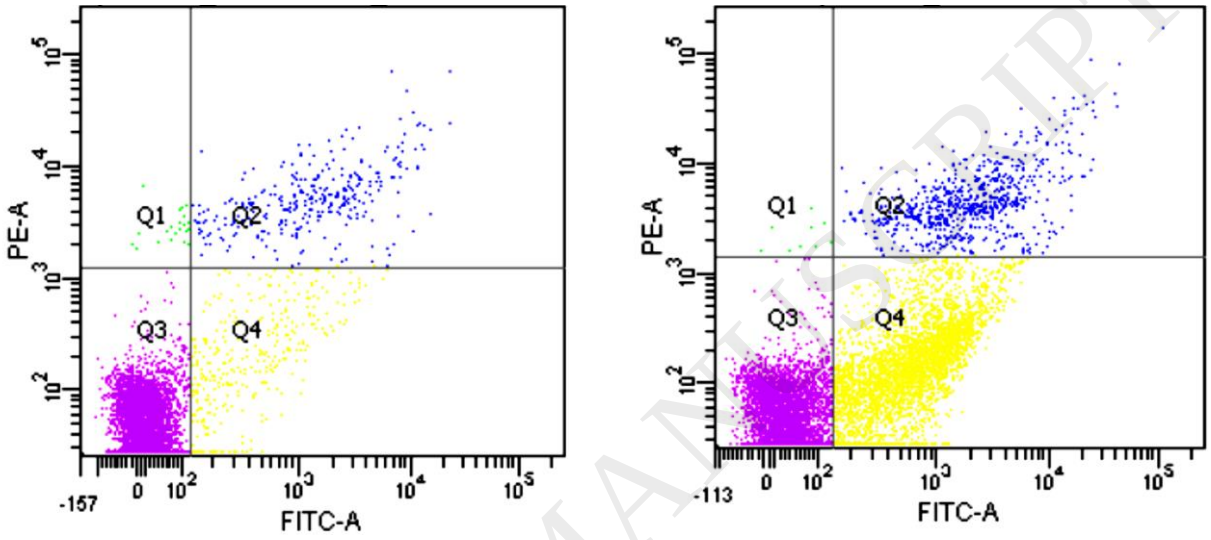

DMSO treated cells (control) **I$_9$** treated cells

Fig. 1. Annexin V-FITC/propidium iodide dual staining assay. RPMI 8226 cells were treated with compound **I$_9$** (7.5 μM) for 72 h, labelled with Annexin V-FITC/PI and examined for apoptosis using flow-cytometer. Cells in the upper left quadrant (Q1): necrotic cells; upper right quadrant (Q2): late apoptotic cells; lower left quadrant (Q3): live cells; lower right quadrant (Q4): early apoptotic cells.

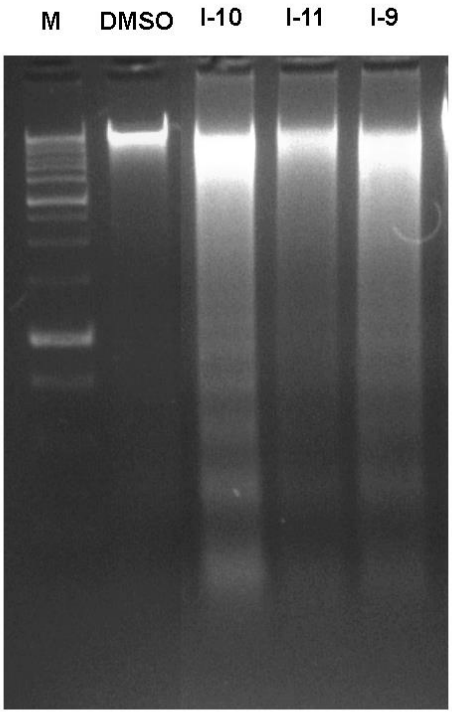

Fig. 2. DNA fragmentations of conjugate DMSO and **I$_9$**–**I$_{11}$** in RPMI 8226 cell line, M is the DNA Marker 50 Kb.

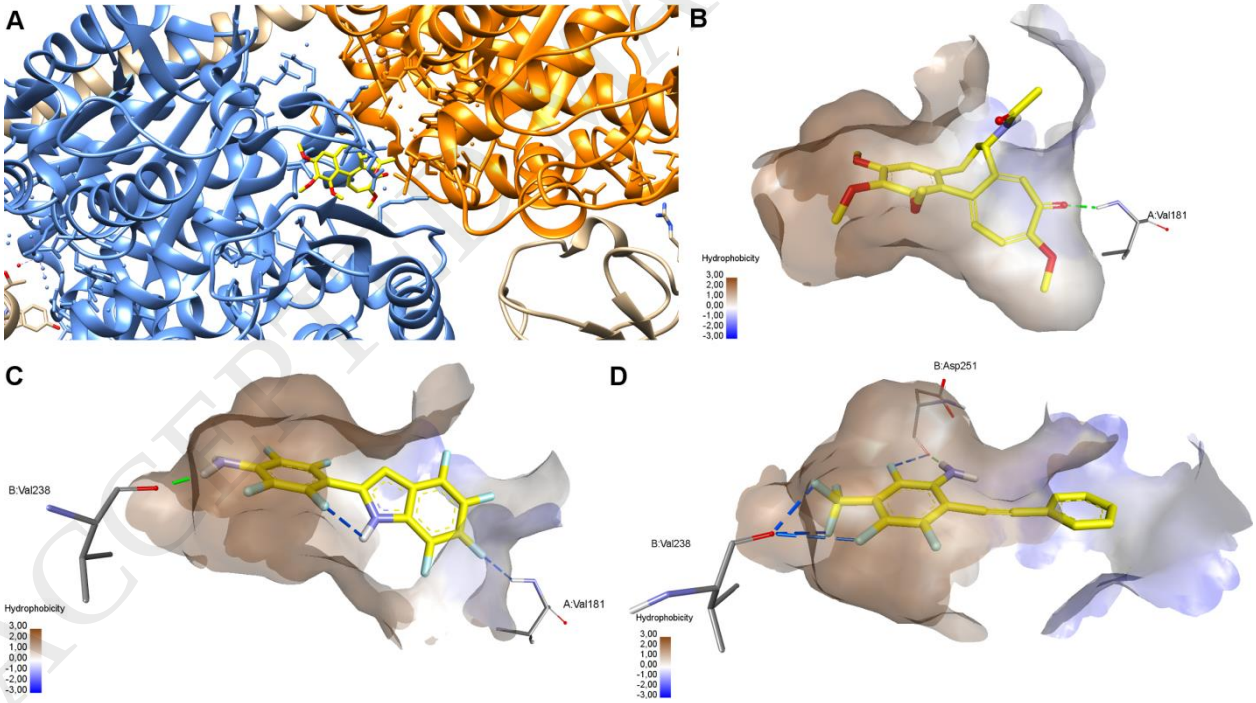

Fig. 3. A: binding site for colchicine on the tubulin surface; secondary structure of chain A is orange, chain B is blue, and the molecule of colchicine is yellow. Noncovalent interactions of molecules in the binding site: B, colchicine; C, **I$_9$**; D, **A$_{13}$**. Hydrophobic interactions are omitted, the surface of the binding site is colored in accordance with the degree of hydrophobicity, and noncovalent interactions are indicated by dashed lines: green, hydrogen bonds; blue, possible weak interactions of fluorine atoms.

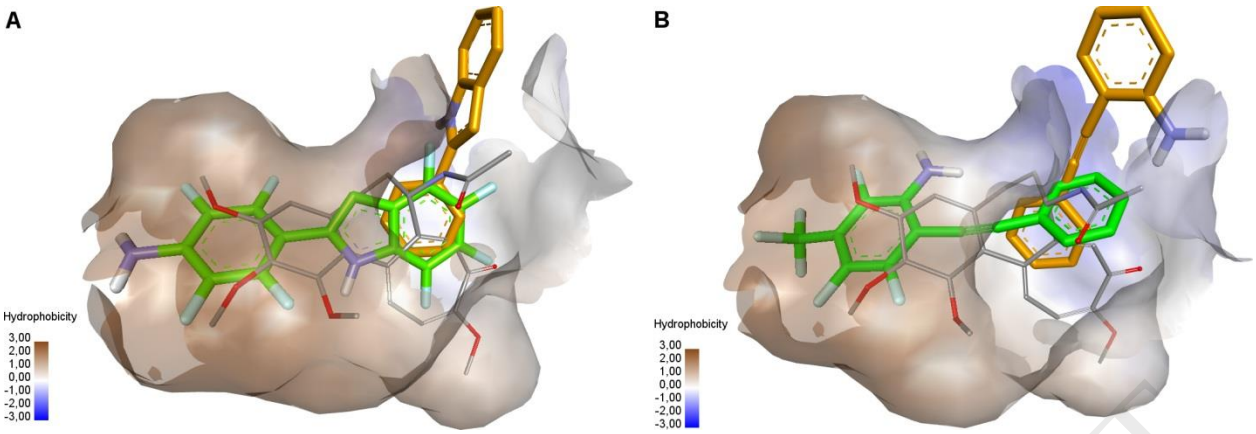

Fig. 4. Superposition of structures in the colchicine-binding site (the surface of the binding site is colored in accordance with the degree of hydrophobicity) on the surface of tubulin. The structures are colored as follows: gray, colchicine; green, **A**$_{13}$ (A) and **I**$_{9}$ (B); orange, **A**$_{18}$ (A) and **I**$_{18}$ (B).

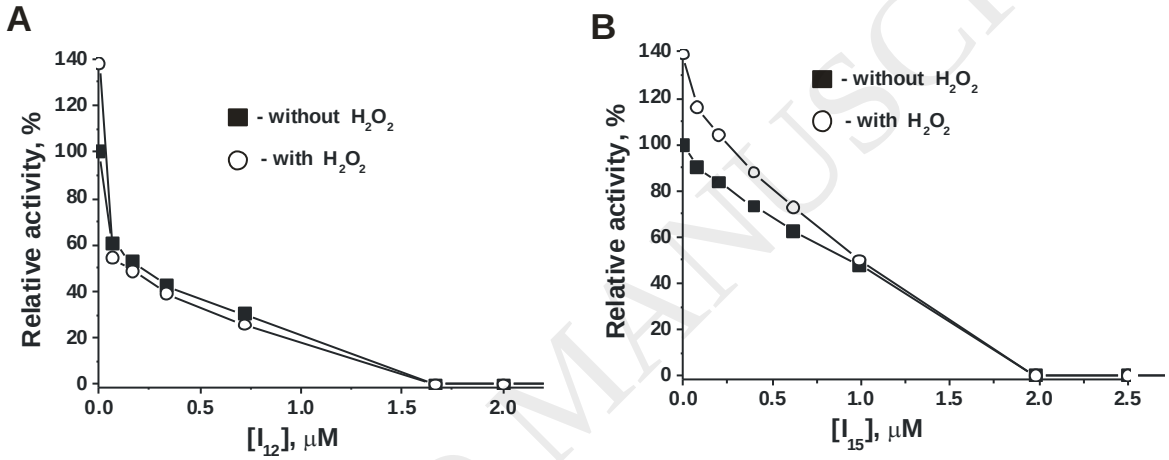

Fig. 5. Analysis of the mutagenic and antioxidant activities of compounds **I**$_{12}$ **(A)** and **I**$_{15}$ (B) by a standard Ames test on *S.* Typhimurium strain TA102 in the absence or presence of 3 mM H_2O_2. The number of revertants in the absence of H_2O_2 was set to 100%. The average error in three experiments for any compound concentration did not exceed 5–10%.

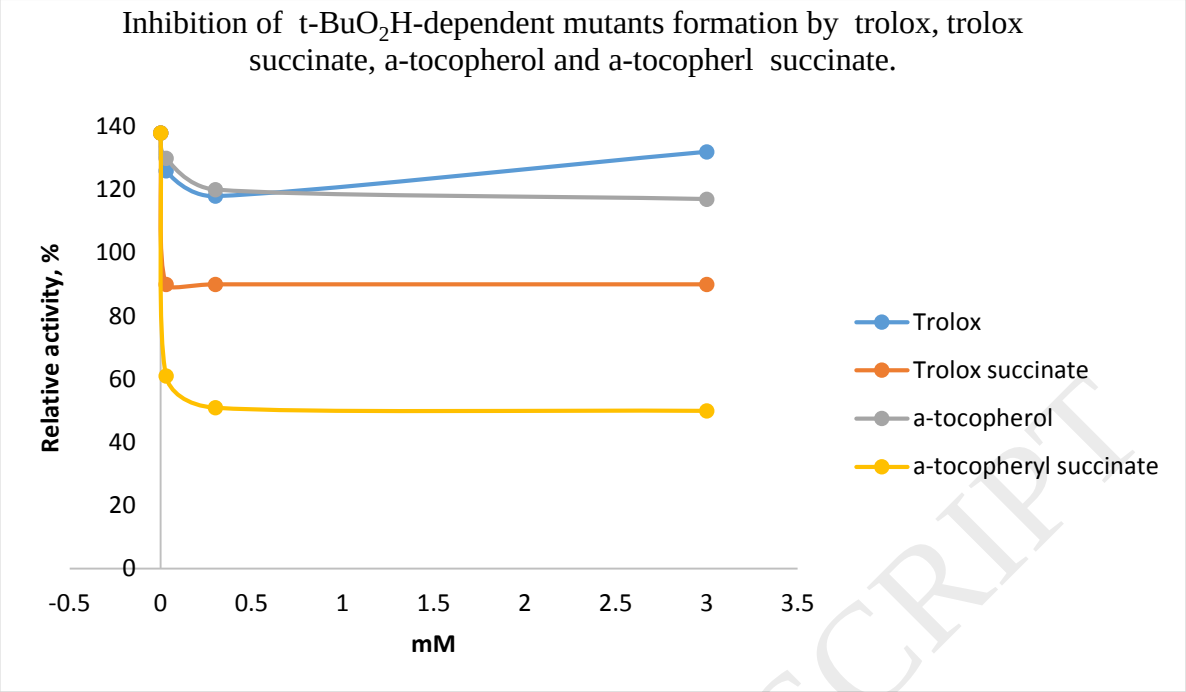

Fig. 6. Analysis of the mutagenic and antioxidant activities of trolox, trolox succinate, tocopherol, tocopheryl succinate by a standard Ames test on *S.* Typhimurium strain TA102 in the absence or presence of 3 mM H_2O_2. The number of revertants in the absence of H_2O_2 was set to 100%. The average error in three experiments for any compound concentration did not exceed 5–10%.

Table 1. *In vitro* cytotoxic activities (IC_{50}, μM) of polyfluorinated diarylacetylenes **A_1–A_{22}** toward cancerous and normal cell lines.

Entry	Compound	Cell viability[a] IC_{50} [μM]							
		MCF-7	RPMI 8226	T98G	HCT 116	HEK 293	WI38	LMTK	AG 17
1	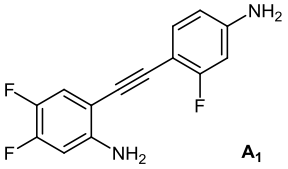 **A_1**	>75	47±2	72±6	>75	>75	74±3	>75	71±5
2	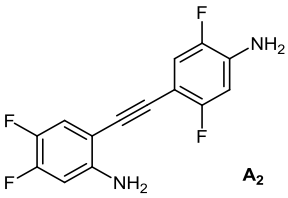 **A_2**	>75	50±3	>75	50±7	72±5	74±3	>75	>75
3	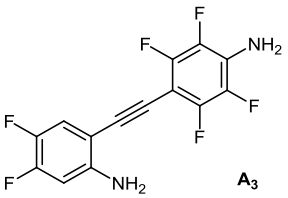 **A_3**	36±5	37±7	68±8	>75	>75	50±9	>75	20±8
4	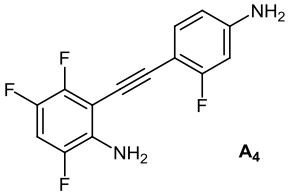 **A_4**	32±7	28±3	40±10	39±7	27±2	31±3	63±4	32±4
5	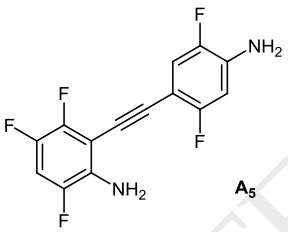 **A_5**	>75	35±3	72±5	>75	>75	73±2	>75	>75
6	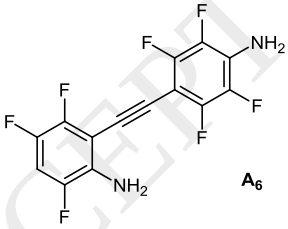 **A_6**	>75	63±4	>75	>75	>75	74±2	>75	72±2
7	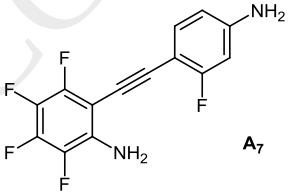 **A_7**	>75	28±2	43±9	66±5	56±6	37±3	>75	>75
8	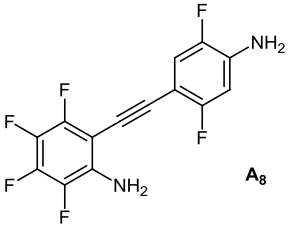 **A_8**	60±10	60±3	73±6	73±6	44±3	52±6	>75	60±5

9	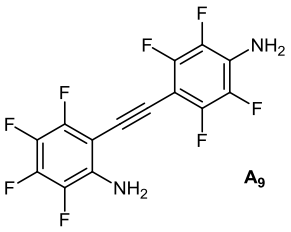 A_9	>75	64±6	>75	>75	>75	72±4	>75	71±6
10	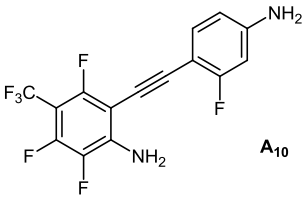 A_{10}	19±6	6±2	24±5	20±2	14±5	21±6	25±4	24±3
11	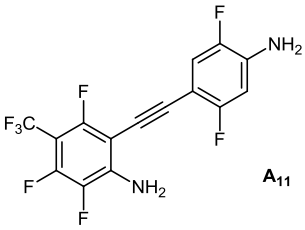 A_{11}	62±9	40±4	66±6	49±2	38±2	36±5	72±6	36±3
12	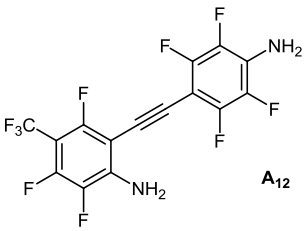 A_{12}	21±5	14±3	34±2	51±7	36±5	34±2	42±5	15±5
13	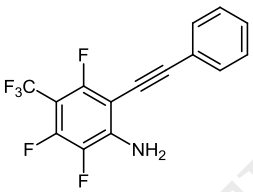 A_{13}	15±4	23±2	40±10	48±7	34±7	23±7	40±6	40±10
14	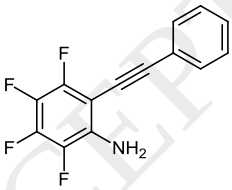 A_{14}	28±7	17±3	>75	53±8	51±7	38±4	35±8	29±5
15	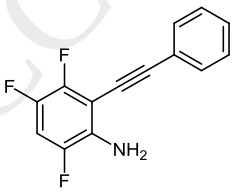 A_{15}	22±8	26±3	52±5	68±6	47±4	39±3	61±5	29±5
16	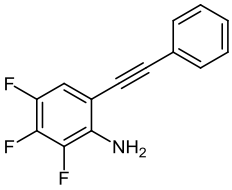 A_{16}	32±2	28±4	46±4	54±3	39±4	29±5	36±5	18±5

17	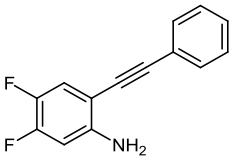 A_{17}	47±8	62±4	>75	>75	72±3	59±5	>75	64±5
18	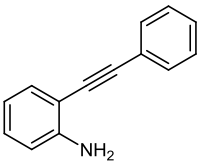 A_{18}	55±5	44±3	63±6	>75	71±4	49±2	>75	46±5

[a] Compound concentration that caused 50% cell growth inhibition (IC_{50}) was determined after 72 h treatment with the indicated compounds. The percentage of viable cells relative to DMSO control (mean ± SD from three independent experiments, each conducted in triplicate) was determined by the MTT assay.

Table 2. *In vitro* cytotoxic activities (IC_{50}, μM) of polyfluorinated indoles **I_1–I_{21}** toward cancerous and normal cell lines.

Entry	Compound	Cell viability[a] IC_{50} [μM]							
		MCF-7	RPMI 8226	T98G	HCT 116	HEK 293	WI38	LMTK	AG 17
1	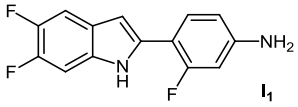 I_1	>75	56±2	49±4	>75	68±5	>75	>75	>75
2	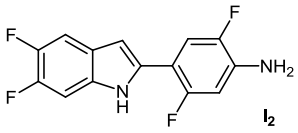 I_2	>75	50±3	>75	>75	55±4	>75	>75	>75
3	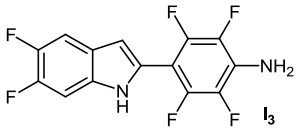 I_3	60±7	ND	>75	ND	38±5	56±3	ND[b]	43±7
4	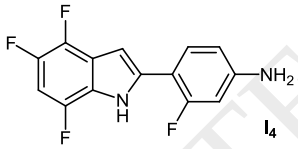 I_4	34±5	8±2	19±6	27±3	20±10	32±4	30±10	27±2
5	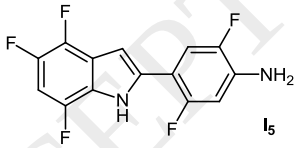 I_5	32±5	24±3	33±9	44±6	49±9	32±5	>75	25±6
6	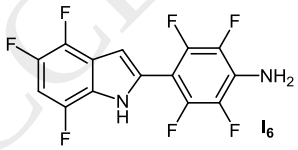 I_6	48±4	28±2	37±3	41±4	35±5	39±1	>75	33±3
7	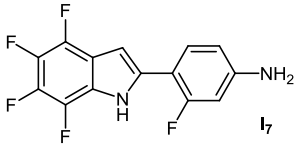 I_7	27±5	10±6	13±4	18±2	20±4	24±4	46±8	19±2
8	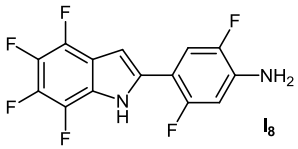 I_8	36±4	7±3	7±10	6±2	2±3	21±1	1±3	25±5

9	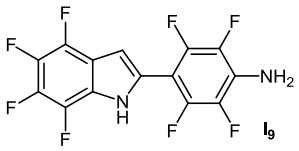 I_9	10±2	3±3	1±1	9±2	4±4	7±2	1±2	6±5
10	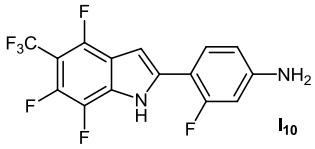 I_{10}	21±5	9±2	12±3	19±4	19±9	24±7	28±4	19±3
11	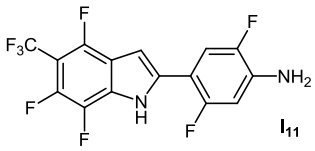 I_{11}	3±3	3±1	5±5	5±1	1±2	3±1	5±2	2±3
12	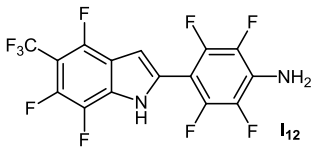 I_{12}	17±4	14±4	25±3	34±9	42±9	26±3	>75	6±3
13	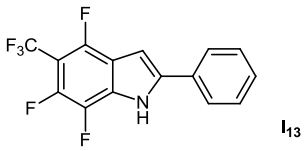 I_{13}	5±4	6±6	11±4	7±4	11±3	10±7	21±8	35±8
14	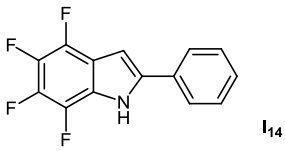 I_{14}	7±7	21±3	20±5	14±2	18±3	18±4	31±5	19±4
15	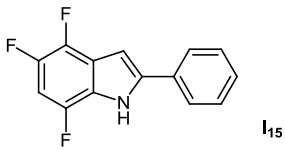 I_{15}	22±8	14±7	25±6	25±2	21±4	23±4	49±5	43±6
16	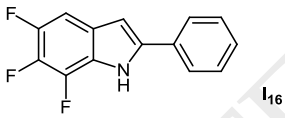 I_{16}	32±4	33±4	45±5	41±4	36±4	38±5	50±4	20±4
17	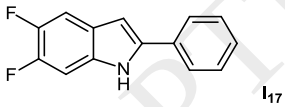 I_{17}	30±6	37±10	72±7	22±5	28±3	>75	ND	>75
18	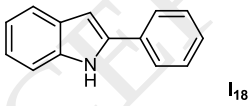 I_{18}	50±2	39±4	1±3	66±5	52±3	>75	ND	60±5
19	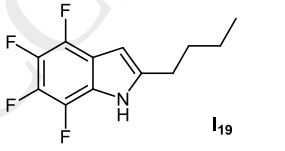 I_{19}	15±10	18±6	28±5	18±2	28±4	17±4	14±2	24±2
20	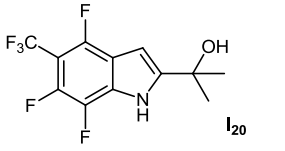 I_{20}	57±4	50±10	50±3	29±4	27±2	47±4	53±7	41±7
21	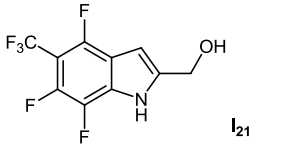 I_{21}	54±7	50±7	52±4	49±4	40±2	49±4	63±5	51±6

22	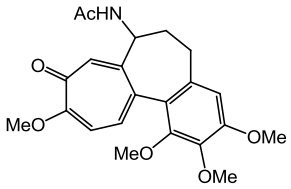	ND[c]	2.2±0.5	0.4±0.5	–	0.1±0.5	–	–	–
	Colchicine (control)								

[a] Compound concentration that caused 50% cell growth inhibition (IC_{50}) was determined after 72 h treatment with the indicated compounds. The percentage of viable cells relative to DMSO control (mean ± SD from three independent experiments, each conducted in triplicate) was determined by the MTT assay.

[b] ND means not effective. Cell viability was equal to or greater than 50% of the DMSO control at 100 μM compound concentration; therefore, accurate IC_{50} values for these compounds were not determined.
[c] See SI.

Table 3. I_9-induces phosphatidylserine exposure. RPMI 8226 cells were treated with 7.5 μM **I_9** for 72 h and analyzed by flow cytometry after annexin V/ PI staining.

Cell population	Cells treated with DMSO	Cells treated with **I_9**
Q1 FITC-/PI+	0.1%	0.1%
Q2 FITC+/PI+	9.4%	7.0%
Q3 FITC-/PI-	78.8%	57.6%
Q4 FITC+/PI-	11.6 %	35.3%

Table 4. Docking scores of the tested compounds with tubulin in the colchicine-, dictyostatin- and vinblastine-binding sites.

Compound	Predicted docking score, kcal/mol		
Control	Colchicine	Dictyostatin	Vinblastin
	-7.49	-6.21	-6.16
I_9	-6.63	-5.12	-4.60
I_{11}	-6.45	-4.34	-4.98
I_{13}	-5.91	-5.00	-5.15
I_{18}	-5.80	-3.88	-4.87
A_{12}	-5.65	-4.97	-3.90
A_{13}	-6.24	-4.38	-5.03
A_{18}	-5.88	-3.84	-4.66

Table 5. IC_{50} values characterizing suppression of spontaneous and H_2O_2-induced mutagenesis by polyfluorinated compounds.

Compound	IC_{50}, μM*		
	Suppression of spontaneous mutagenesis (from 100% to 50%)	Suppression of H_2O_2-induced and spontaneous mutagenesis	
		From 138% to 100%	From 100% to 50%
A_2	1.21±0.01	0.050±0.003	0.93±0.04
A_5	1.31±0.01	0.060±0.004	1.0±0.06
A_{10}	0.72±0.05	0.043±0.002	0.52±0.03
A_{12}	0.72±0.04	0.037±0.002	0.72±0.03
I_2	1.00±0.07	0.053±0.003	0.78±0.04
I_4	0.43±0.02	0.057±0.003	0.75±0.03
I_7	0.60±0.04	0.074±0.004	0.77±0.04
I_9	0.71±0.05	0.037±0.002	0.43±0.02
I_{10}	0.63±0.03	0.037±0.002	0.37±0.02
I_{11}	0.76±0.05	0.030±0.001	0.57±0.03
I_{12}	0.22±0.01	0.028±0.001	0.16±0.01
I_{14}	0.94±0.06	0.049±0.002	1.10±0.05
I_{15}	0.94±0.05	0.25±0.001	1.0±0.06
I_{17}	1.18±0.07	0.079±0.004	1.1±0.05
I_{19}	1.34±0.08	0.073±0.003	0.86±0.04
I_{20}	0.34±0.02	0.040±0.002	0.13±0.01
I_{21}	0.71±0.05	0.056±0.004	0.78±0.03

*Mean ± S.D. from three independent experiments.